ANALYTICAL AND NUMERICAL ANALYSIS OF ELECTRON TRAJECTORIES IN A 3-D UNDULATOR MAGNETIC FIELD*

N.V. Smolyakov#, S.I. Tomin, NRC Kurchatov Institute, Moscow, Russia
G. Geloni, European XFEL GmbH, Hamburg, Germany

Abstract

It is well-known that an electron trajectory in an undulator is influenced by the magnetic field focusing properties (both horizontal and vertical). Approximate solutions of the equations of motion for electrons in a 3-dimensional magnetic field, which describes these focusing properties, are usually found, in literature, by means of averaging over the short-length oscillations. At variance, the equations of motion can be solved numerically, for example by applying the Runge-Kutta algorithm. It is shown in this paper that there are cases where the numerically computed trajectories, which can be considered, for our purposes, as exact, differ considerably from the corresponding approximate solutions obtained through the averaging method. This means that the undulator field influence on the electron trajectory is complicated and that approximations found in literature should be used with extreme care.

INTRODUCTION

As far as we know, horizontal and vertical focal lengths of an undulator were first calculated in [1]. In a planar undulator with infinitely wide magnetic poles and hence without horizontal focusing, the vertical focusing was analysed in [2, 3]. In [4, 5] trajectories in the presence of focusing undulator magnetic field were calculated up to the lowest order in the initial positions and angles of the electrons. Some general relations dealing with undulator focal lengths were derived in [6 – 8]. Long-length-scale anharmonic betatron motion of electrons in very long undulators was studied in [9]. All these studies were carried out within the following limits: the focusing effects were calculated averaging over the undulator period and only terms, which are linear in the electron initial positions and angles, were taken into account.

In this paper we discuss the limits of this approximation when one needs to calculate the electron trajectory with high accuracy. Consider, for example, the line width of FEL radiation, which is related to the dimensionless Pierce parameter ρ. It has typical values for XFELs of the order of 10^{-4}. Since an accuracy of the fundamental wavelength is about $\Delta\lambda/\lambda \le \rho$, the requirement on the accuracy for the undulator deflection parameter K is very strict, $\Delta K \approx 10^{-4}$. The expression for the phase of spontaneous radiation in the general case [10] gives the following relation for K, see Fig. 1:

$$\frac{K^2}{2} = \frac{\gamma^2}{\lambda_u}\int_0^{\lambda_u} \beta_x^2(z)dz\,. \qquad (1)$$

Here λ_u is an undulator period, γ is an electron reduced energy, β_x is its reduced horizontal velocity, being of the order of K/γ. It can be derived from (1) that the necessary accuracy for β_x is of the order of $\Delta\beta_x \approx \Delta K/\gamma \approx 3\cdot 10^{-9}$. It is doubtful whether known analytical (approximate) solutions for trajectories, obtained with the averaging method, provide so high accuracy. In fact, we will show in this article that they should be used with extreme care.

TRAJECTORY EQUATIONS IN 3-D FIELD

We model the three-dimensional magnetic field by the following expressions which satisfy Maxwell equations:

$$B_x(x,y,z) = -\frac{k_x}{k_y}B_0\sin(k_x x)\sinh(k_y y)\sin(k_z z)\,, \qquad (2)$$

$$B_y(x,y,z) = B_0\cos(k_x x)\cosh(k_y y)\sin(k_z z)\,, \qquad (3)$$

$$B_z(x,y,z) = \frac{k_z}{k_y}B_0\cos(k_x x)\sinh(k_y y)\cos(k_z z)\,. \qquad (4)$$

Here $k_x = 1/a$, $k_z = 2\pi/\lambda_u$, $k_y = \sqrt{k_x^2 + k_z^2}$, λ_u is the undulator period length. The linear parameter a gives the field non-uniformity along X-axis and is of the order of the width of the undulator poles.

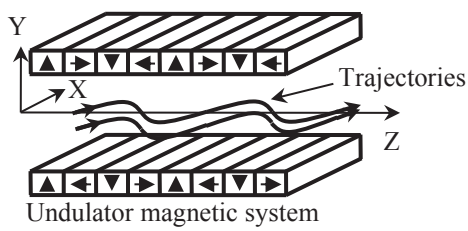

Figure 1: Sketch of a permanent magnet undulator.

We will use the exact equations for trajectory [11]:

$$x'' = -q\sqrt{1+x'^2+y'^2}\left\{(1+x'^2)B_y - y'B_z - x'y'B_x\right\}, \qquad (5)$$

$$y'' = q\sqrt{1+x'^2+y'^2}\left\{(1+y'^2)B_x - x'B_z - x'y'B_y\right\}. \qquad (6)$$

Here β and γ are the electron reduced velocity and energy respectively, $q = e/(mc^2\beta\gamma)$ and an apostrophe indicates a derivative with respect to z.

A computer code was written, which solves the systems of Eqs. (2) – (6) by using the Runge-Kutta algorithm.

*This work was partially supported by the Russian Federation program "Physics with Accelerators and Reactors in West Europe (except CERN)" and by BMBF-Project 05K12GU2.
smolyakovnv@mail.ru

ISBN 978-3-95450-126-7

FOCUSING SOLUTION

By neglecting all quadratic in x, x', y and y' terms in Eqs. (5) and (6), we get the electron trajectory:

$$x_1(z) = x_0 + \theta_0 z - (p/k_z)\sin(\varphi), \quad (7)$$

$$y_1(z) = y_0 + y_0' z. \quad (8)$$

Here $K = (eB_0\lambda_u)/(2\pi mc^2)$ is an undulator deflection parameter, $p = K/(\beta\gamma)$, $\theta_0 = x_0' + p$ and $\varphi = k_z z$.

We may generalize these expressions, searching for "focusing" solutions for Eqs. (5) and (6) in the form:

$$x_f(z) = x_s(z) - (p/k_z)\sin(\varphi), \quad (9)$$

$$y_f(z) = y_s(z), \quad (10)$$

where $x_s(z)$ and $y_s(z)$ are slowly varying functions. Substituting Eqs. (9) and (10) into (5) and (6), and averaging over the undulator period (thus cancelling the fast oscillating terms), we get the following equations found in previous works [4] and [5]:

$$x_s''(z) - k_z^2\omega_x^2 x_s(z) = 0, \quad (11)$$

$$y_s''(z) + k_z^2\omega_y^2 y_s(z) = 0, \quad (12)$$

where $\omega_x = (pk_x)/(\sqrt{2}k_z)$ and $\omega_y = (pk_y)/(\sqrt{2}k_z)$ are the dimensionless betatron oscillations periods in units of λ_u along the horizontal and the vertical directions. Solving these equations, we get for $x_f(z)$ and $y_f(z)$:

$$x_f(z) = x_0\cosh(\omega_x\varphi) + \frac{\theta_0}{\omega_x k_z}\sinh(\omega_x\varphi) - \frac{p}{k_z}\sin(\varphi), \quad (13)$$

$$y_f(z) = y_0\cos(\omega_y\varphi) + \frac{y_0'}{\omega_y k_z}\sin(\omega_y\varphi), \quad (14)$$

The main result of this paper is to point out that although relations (13) and (14) have been universally accepted, in some practically important cases they may be in sharp contrast with more accurately calculated results. Therefore, Eqs. (13) and (14) should be used carefully.

NUMERICAL SIMULATIONS

Let us compare the trajectory computed numerically via the Runge-Kutta algorithm (marked as "RK") with those given by Eqs. (13) and (14) (marked as "focus").

Since focusing effects are much smaller than linear parts of trajectory x_1 and y_1 (see (7), (8)), we will extract x_1 and y_1 from trajectories x_{RK}, y_{RK}, x_f and y_f:

$$\Delta X_{RK} = x_{RK}(z) - x_1(z), \quad \Delta Y_{RK} = y_{RK}(z) - y_1(z),$$

$$\Delta X_{focus} = x_f(z) - x_1(z), \quad \Delta Y_{focus} = y_f(z) - y_1(z).$$

We will consider here two simplest examples, namely, electrons moving along a single undulator segment with initial zero horizontal shift and zero horizontal deflections relative to the equilibrium trajectory: $x_0 = 0$ and $\theta_0 = 0$, while the vertical initial coordinates are equal to $\{y_0 = 0.03\,mm, y_0' = 0\}$ and $\{y_0 = 0, y_0' = 0.002\,mrad\}$ (Figs. 2 – 4 and Figs. 5 – 7 correspondingly).

The simulations were performed with the European XFEL parameters listed in the Table 1 (see [12]).

Table 1: European XFEL Parameters for Simulation

Electron beam energy	17.5 GeV
Normalized emittance ε_n	10^{-6} m rad
RMS beam emittance $\varepsilon = \varepsilon_n/\gamma$	$2.9*10^{-11}$ m rad
Averaged beta-function	15 m
Undulator period λ_u	40 mm
Undulator deflection parameter K	4
Horizontal non-uniformity a	50 mm
Number of undulator periods N	124

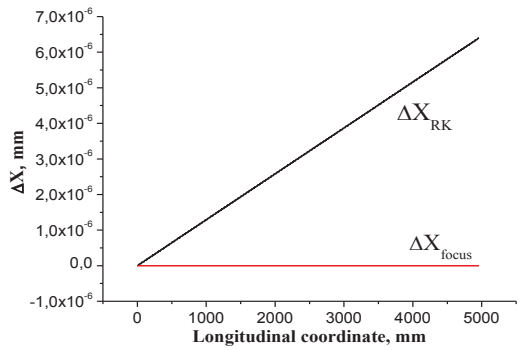

Figure 2: Analytically calculated ΔX_{focus} (red line) vs. numerically simulated ΔX_{RK} (black curve) horizontal coordinates of trajectories with $\{y_0 = 0.03\,mm, y_0' = 0\}$.

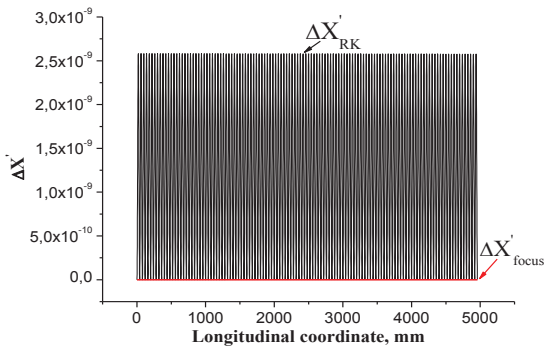

Figure 3: Analytically calculated $\Delta X'_{focus}$ (red line) vs. numerically simulated $\Delta X'_{RK}$ (black curve) horizontal velocities of trajectories with $\{y_0 = 0.03\,mm, y_0' = 0\}$.

We mention that $\Delta X_{focus} = \Delta X'_{focus} = 0$ for this case (red lines), while numerical simulations show non-zero horizontal shift of trajectory. It can be easily estimated from Fig. 3 that the average horizontal velocity is about $1.3*10^{-9}$, giving about $1.3*10^{-9}*4960=6.448*10^{-6}$ mm horizontal shift at the 4960 mm undulator length (Fig 2).

ISBN 978-3-95450-126-7

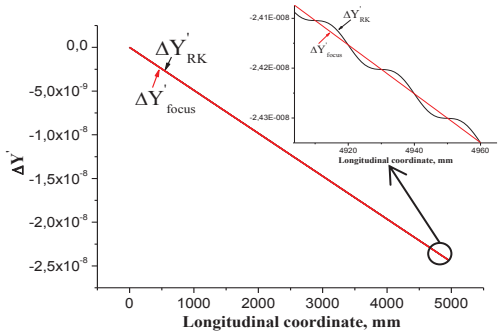

Figure 4: Analytically calculated $\Delta Y'_{focus}$ (red curve) vs. numerically simulated $\Delta Y'_{RK}$ (black curve) vertical velocities of trajectories with $\{y_0 = 0.03\ mm,\ y'_0 = 0\}$.

Figs. 5 - 7 show the electron trajectories with the initial coordinates $x_0 = \theta_0 = y_0 = 0$, $y'_0 = 0.002\ mrad$.

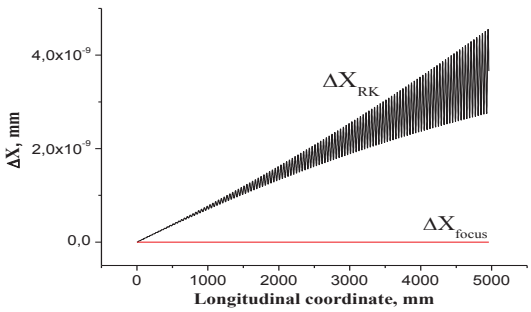

Figure 5: Analytically calculated ΔX_{focus} (red line) vs. numerically simulated ΔX_{RK} (black curve) horizontal coordinates of trajectories with $\{y_0 = 0,\ y'_0 = 0.002\ mrad\}$.

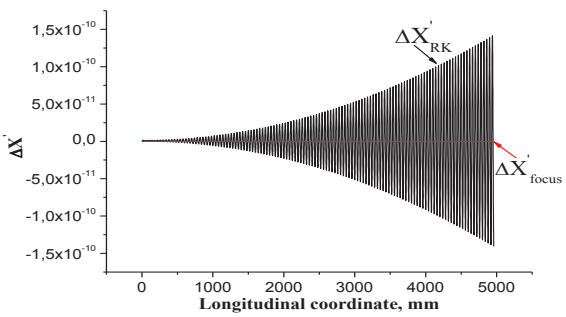

Figure 6: Analytically calculated $\Delta X'_{focus}$ (red line) vs. numerically simulated $\Delta X'_{RK}$ (black curve) horizontal velocities of trajectories with $\{y_0 = 0,\ y'_0 = 0.002\ mrad\}$.

Figs. 2, 3, 5 and 6 show that initial shift and deflection of electrons in the vertical direction result in additional horizontal oscillations of electron velocities, about $2.5 \cdot 10^{-9}$ in amplitude in our case.

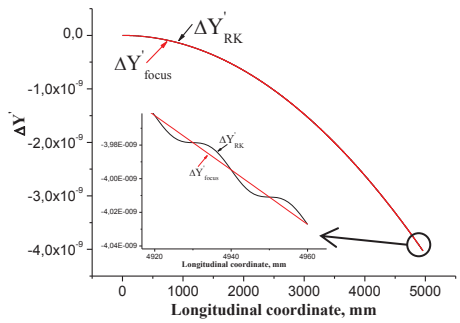

Figure 7: Analytically calculated $\Delta Y'_{focus}$ (red curve) vs. numerically simulated $\Delta Y'_{RK}$ (black curve) vertical velocities of trajectories with $\{y_0 = 0,\ y'_0 = 0.002\ mrad\}$.

Figs. 4 and 7 show that Eq. (14) gives relatively small errors for vertical components of trajectory, see also [13].

Note that Eqs. (2-6) can also be approximately solved by means of a perturbation theory approach, which allows one to find analytical results with higher accuracy than (13) and (14); preliminary results are published in [14], and more extended studies will be the subject for future works. These analytical results, whilst much more sophisticated compared with Eqs. (13) and (14), are in excellent agreement with those computed numerically with the help of the Runge-Kutta algorithm, also confirming the numerical results presented here.

ACKNOWLEDGMENT

We would like to thank M. Rychev, S. Molodtsov and V. Nosik for supporting this direction of research.

REFERENCES

[1] L.M. Barkov et al., Nucl. Instr. Meth. 152 (1978) 23.
[2] R.P. Walker, Nucl. Instr. Meth. 214 (1983) 497.
[3] P. Torggler and C. Leubner, Phys. Rev. A39 (1989) 1989.
[4] G. Dattoli and A. Renieri, "Experimental and Theoretical Aspects of the Free-Electron Laser," *Laser Handbook v. 4,* ed. M.L. Stitch and M. Bass (North-Holland, 1985).
[5] E.T. Scharlemann, J. Appl. Phys. 58 (1985) 2154.
[6] N.V. Smolyakov, Nucl. Instr. Meth. A308 (1991) 83.
[7] N.V. Smolyakov, Sov. Phys. Tech. Phys. 37 (1992) 309.
[8] P. Elleaume, Rev. Sci. Instrum. 63 (1992) 321.
[9] J.J. Barnard, Nucl. Instr. Meth. A296 (1990) 508.
[10] N.V. Smolyakov, "Shift-Scale Invariance of Electromagnetic Radiation," *Electromagnetic Radiation,* ed. S.O. Bashir (INTECH, 2012); http://www.intechopen.com/books/electromagnetic-radiation/shift-scale-invariance-of-electromagnetic-radiation

ISBN 978-3-95450-126-7

[11] K.Steffen, "Fundamentals of Accelerator Optics Synchrotron Radiation and Free Electron Lasers," Proc. CAS CERN Acceler. School ed S. Turner (CERN 90-03), p. 1 (Geneva, 1990).
[12] Th. Tschentscher, "Layout of the X-Ray Systems at the European XFEL," XFEL.EU TN-11-001 (2011).
[13] N. Smolyakov , S. Tomin, G. Geloni, "Electron Trajectories in a Three-Dimensional Undulator Magnetic Field," IPAC2013, Shanghai, China, May 2013, WEPWA044, p. 2223 (2013); http://accelconf.web.cern.ch/AccelConf/IPAC2013/papers/wepwa044.pdf
[14] N. Smolyakov, S. Tomin, G. Geloni, J. Phys.: Conf. Ser. 425 (2013) 032023; http://iopscience.iop.org/1742-6596/425/3/032023

ISBN 978-3-95450-126-7